Monatshefte für Chemie 131, 1139–1150 (2000)

Monatshefte für Chemie
Chemical Monthly

Catalytic Decomposition of H_2O_2 over Supported ZnO

Ibrahim A. Salem*

Chemistry Department, Faculty of Science, United Arab Emirates University, Al-Ain, United Arab Emirates

Summary. Transition metal sulfates of Cu(II), Co(II), Ni(II), Cr(III), Mn(II), and Fe(III) supported on ZnO were prepared and characterized by SEM, EDX, and XRD. The kinetics of the heterogeneous decomposition of H_2O_2 over these supported catalysts was investigated. The reaction rate is correlated with both the amount of supported metal ion and its redox potential. The rate of reaction increases with increasing initial concentration of H_2O_2, attains a maximum, and decreases thereafter. It also increases with *pH* and reaches a maximum at high *pH* values. A reaction mechanism is proposed that implies the formation of a peroxo intermediate at the early stages of the reaction. A second intermediate is assumed to be formed at high $[H_2O_2]_o$ which inhibits the progress of the reaction.

Keywords. Hydrogen peroxide; Zinc oxide; Transition metal ions; Decomposition; Kinetics; Catalysts.

Introduction

In recent years, hydrogen peroxide has attracted increasing attention as a promising oxidant for the removal of toxic pollutants from water [1–9]. It is also used for removing color from dye baths, thus facilitating dye bath reuse in textile industry [10–13]. The basic idea of using hydrogen peroxide for such processes depends on the fact that its catalytic decomposition release highly active and non-specific hydroxyl radicals [1–16] which oxidize many organic pollutants with rate constants ranging from 10^8 to $10^{10}\,M^{-1}\cdot s^{-1}$ and mineralize them to CO_2 and H_2O owing to their high oxidation potential ($E^o = +2.8$ V) [9, 12]. Hydrogen peroxide is referred to as a friendly oxidant in environmental processes since the only byproducts formed are oxygen and water. The catalytic decomposition of hydrogen peroxide has been performed both in homogeneous and heterogeneous media. Generally, homogeneous catalysts are very efficient, but their recovery from the treated effluents is difficult and brings about additional costs. This problem as well as the isolation of the reaction products can be overcome by using heterogeneous catalysts.

The heterogeneous decomposition of aqueous hydrogen peroxide over supported metal ions, metal oxides, and metal complexes has been the subject of

* Permanent address: Chemistry Department, Faculty of Science, Tanta University, Tanta, Egypt

many investigations. Polymers [17], cation exchange resins [18], alumina [19], silica gel [20], silica [21], silica-alumina mixtures [22], clays [23], and zirconia [24] have been used as supports for transition metal ions and/or their complexes. The catalytic activity of these catalysts towards H_2O_2 has been found to be strongly dependent on surface area, redox potential of the supported metal ions, basicity of the complexed ligands, and DVB% of the resins. With supported zirconia, the reaction rate increased with increasing *pH*, attaining a limiting rate at high *pH* values [24]. Metal oxides have also been used as potentially active catalysts with respect to hydrogen peroxide decomposition [25–32]. Their catalytic activity depends considerably on the method of preparation [25–27]. Mixing oxides of cobalt, bismuth, and chromium with MnO_2 greatly affects the latter's catalytic activity [30, 31]. However, pure and Li_2O doped Co_3O_4 with different amounts of dopant also activate the decomposition of H_2O_2 [32].

On the other hand, zinc oxide, metal ions supported on zinc oxide, and zinc oxide mixed with other oxides have been prepared and used as active catalysts for the oxidation of inorganic and organic compounds [33–36]. Appropriate catalytic activity and high selectivity to mineralization products were found for the oxidation of pentachlorophenol on zinc oxide [33]. Mixing ZnO with CuO and/or Al_2O_3 in different ratios showed a high activity towards the oxidation of carbon monoxide, phenols, 2-propanol, and some industrial waste water effluents [34–36].

The present work, which is part of a project concerning environmental catalysis, reports the kinetics of the heterogeneous decomposition of H_2O_2 using some transition metal ions supported on zinc oxide as active catalysts. One of its objectives is to examine and compare the activity of these catalysts towards H_2O_2 decomposition in conjunction with the oxidative degradation and color removal of some organic dyes from industrial waste effluents.

Results and Discussions

Catalyst characterization

Figure 1 shows the SEM micrographs of pure ZnO and ZnO loaded with metal ions. Differences in apparent porosity, shape, and particle size can be noted. Generally, the particle size increases upon supporting ZnO with metal ions, and the degree of increase depends on the loaded metal ion. Greater particle size is observed for Cu^{2+} and Co^{2+} and, to a minor extent, for Cr^{3+}, Mn^{2+}, Ni^{2+} and Fe^{3+}. As particle size increases, the porosity increases and the surface area decreases. The data in Table 1 show the EDX measurements recorded for the different catalysts as well as for pure ZnO. The data clearly demonstrate that the amount of Cr^{3+} on the catalyst surface is greater than that of the other metal ions. For the ZnO/Ni^{2+} catalyst, despite the amount of Ni^{2+} loaded onto ZnO is very low compared to either Co^{2+} or Fe^{3+}, the surface content is almost equal to that of Co^{2+} and little bit lower than that of Fe^{3+}. This suggests that most of the Ni^{2+} ions are present on the catalyst surface. The very low amount of Mn^{2+} on the surface is attributed to the low affinity of ZnO towards Mn^{2+} ions (1.27 mg Mn^{2+}/g ZnO).

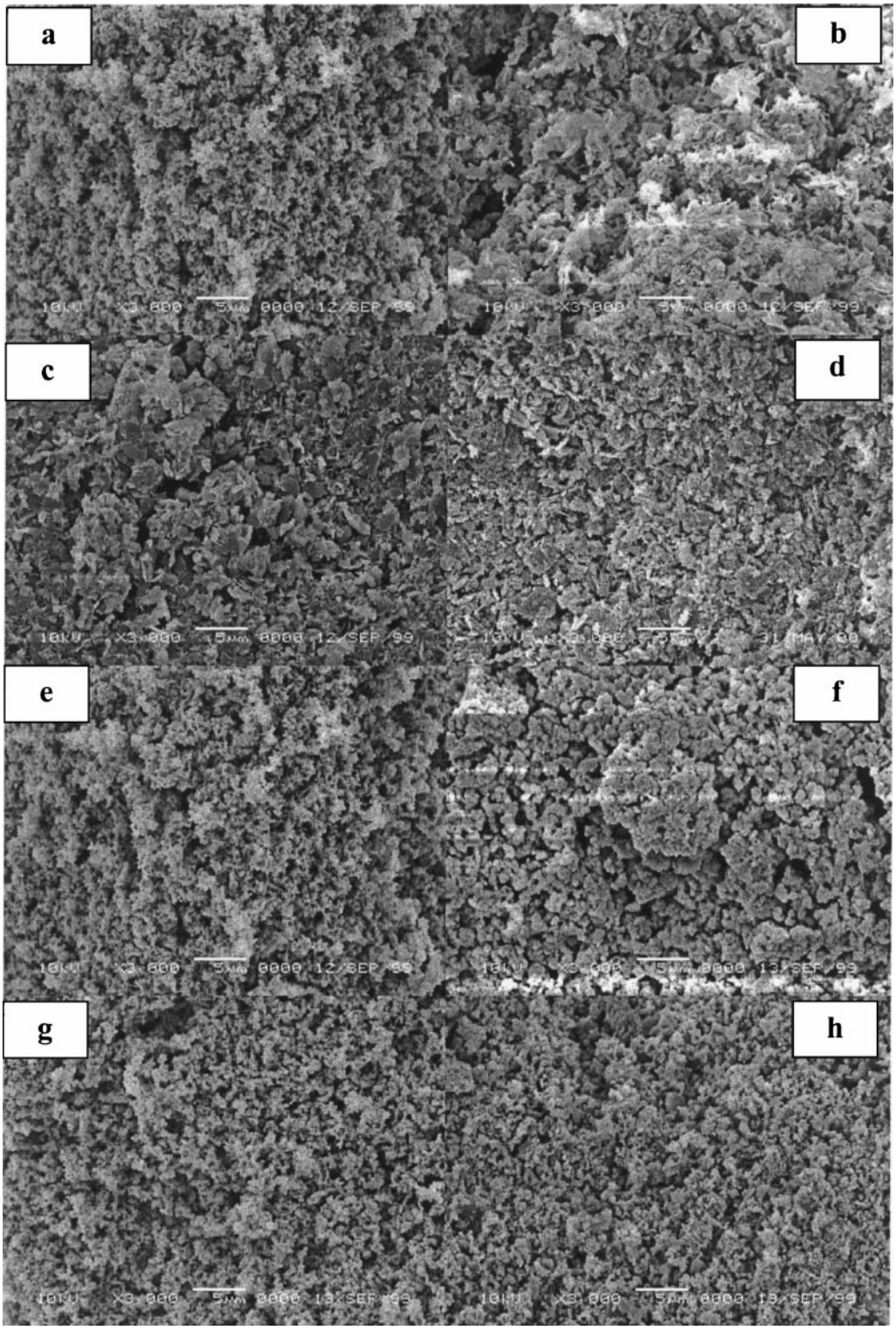

Fig. 1. SEM micrographs for unsupported (a, e) and supported ZnO with (b) Cu^{2+}, (c) Co^{2+}, (d) Ni^{2+}, (f) Cr^{3+}, (g) Mn^{2+}, and (h) Fe^{3+}

Table 1. EDX and atomic absorption measurements together with the color of the different catalysts before and after the reaction with 0.20 *M* hydrogen peroxide

Catalyst	EDX				mg M^{n+} / g catalyst	Start of reaction	During reaction
	O %	S %	M^{n+} %	Zn %			
ZnO	11.22	–	–	88.78	–		
$ZnO/CuSO_4$	18.38	2.06	4.86	74.71	65.22	blue	brown
ZnO/CuO[a]	4.78	–	8.84	86.39	–	green	brown
$ZnO/CoSO_4$	9.17	1.31	7.44	82.08	46.77	pink	faint pink
$ZnO/NiSO_4$	18.84	2.31	7.25	71.60	11.45	green	green
$ZnO/Cr_2(SO_4)_3$	27.87	2.46	16.93	52.75	168.36	gray	yellowish green
ZnO/Cr_2O_3[a]	15.94	–	18.53	65.53	–	black	black
$ZnO/MnSO_4$	15.24	0.04	0.11	84.61	1.27	dirty white	dirty white
$ZnO/Fe_2(SO_4)_3$	25.86	2.73	9.55	61.87	59.78	faint brown	faint brown

[a] Calcinated for three hours at 500°C

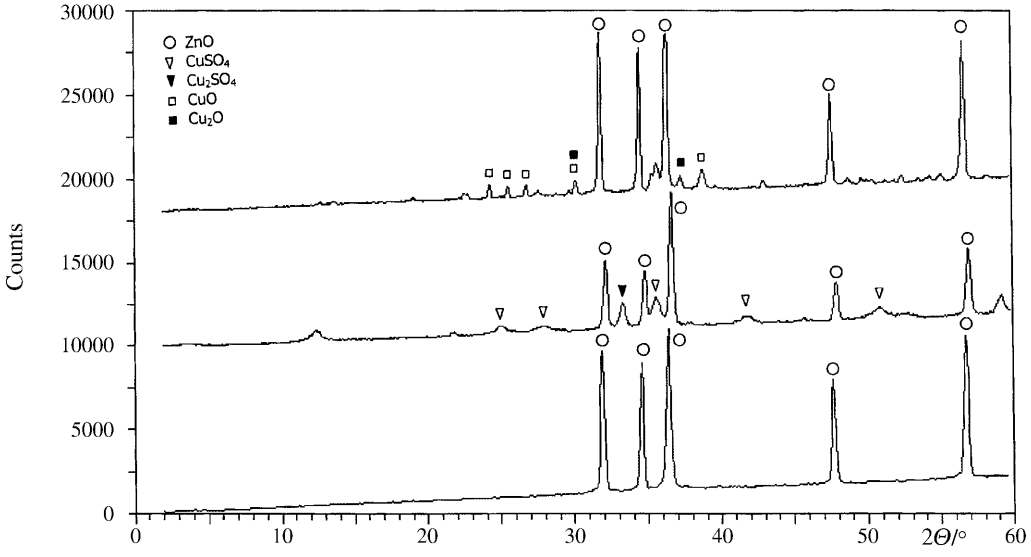

Fig. 2. X-Ray diffraction for (a) ZnO, (b) ZnO/Cu^{2+}, and (c) ZnO/Cu^{2+} after calcination at 500°C

The identity of the support is revealed by the corresponding XRD pattern (Fig. 2) which shows a series of reflections typical for zincite (curve a). The addition of copper(II) sulfate to zincite results in the formation of two new phases, mainly $CuSO_4$ and, to a little extent, Cu_2SO_4. The intensity of the reflections corresponding to zincite is suppressed by the formation of these new phases (curve b). Calcination

of the latter produces new diffraction peaks corresponding to the formation of mixed phases of CuO (major) and Cu_2O (minor) (curve c). This is accompanied by an enhancement of the diffraction peaks corresponding to zincite.

Reaction with hydrogen peroxide

A very slow decomposition of H_2O_2 was observed over pure zinc oxide. However, when ZnO was loaded with a transition metal ion, *e.g.* Cu^{2+}, Co^{2+}, Mn^{2+}, Cr^{3+}, Fe^{3+}, or Ni^{2+}, a higher reaction rate was observed. The order of reactivity depends strongly on the initial concentration of hydrogen peroxide, $[H_2O_2]_o$ (Fig. 3). At $[H_2O_2]_o < 1$ *M* the reaction rate increases in the following order: $Cr^{3+} > Cu^{2+} > Fe^{3+} > Mn^{2+} > Co^{2+} > Ni^{2+}$ (Fig. 3). This order is correlated with both the redox potential and the amount of loaded metal ion [24, 37]. The net effect depends on which of these factors is the most pronounced. For example, comparing Cu^{2+} with Cr^{3+}, despite the fact that the redox potential of Cu^{2+} is greater than that of Cr^{3+} [37], the rate with Cr^{3+} is greater than that with Cu^{2+} because of the higher amount of supported Cr^{3+} (Tables 1 and 2). Similarly, the higher rate with Cr^{3+} compared to Fe^{3+} can be ascribed to the greater amount of metal ion loaded. The low rate observed with Mn^{2+}, Ni^{2+}, and Co^{2+} is in agreement with their redox potential [37]. However, at $[H_2O_2]_o > 1$ *M*, the order of reactivity is changed.

Inspection of Fig. 3 reveales that the reaction rate first increases gradually with increasing $[H_2O_2]_o$, reaches a maximum, and then decreases. This is ascribed to the formation of an intermediate active species which exerts an inhibiting effect on the reaction rate [22, 24]. However, at high $[H_2O_2]_o$, the latter can be transformed to a second intermediate which greatly decreases the reaction rate.

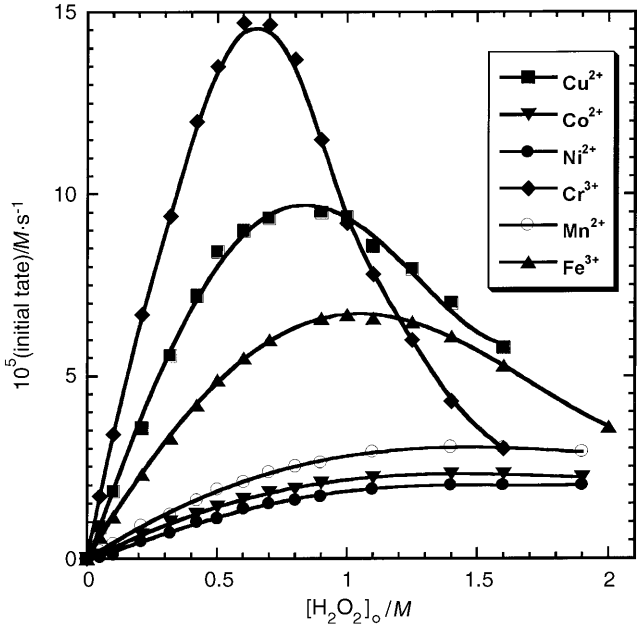

Fig. 3. Variation of the initial reaction rate with the initial concentration of hydrogen peroxide for its reaction with one gram of ZnO loaded with transition metal ions at $pH = 8.15$ and 35°C

Table 2. Rate constants and activation parameters for the reaction of 2 g of the different catalysts with 0.42 M H_2O_2 at $pH = 8.15$

Catalyst	$10^4 k_{obs}/s^{-1}$				Activation parameters			
	25°C	30°C	35°C	40°C	E_a / kJ · mol^{-1}	$\Delta G^{\#}$ / kJ · mol^{-1}	$\Delta H^{\#}$ / kJ · mol^{-1}	$\Delta S^{\#}$ / J · deg^{-1} · mol^{-1}
$ZnO/CuSO_4$	0.61	1.08	1.75	3.08	79.3	97.43	76.8	−67.5
ZnO/CuO[a]	0.90	1.52	2.40	4.01	76.01	96.60	73.47	−75.71
$ZnO/CoSO_4$	0.11	0.19	0.29	0.47	72.01	101.5	69.46	−105
$ZnO/NiSO_4$	0.17	0.21	0.26	0.37	45.12	101.9	42.58	−194
$ZnO/Cr_2(SO_4)_3$	1.19	1.95	2.86	4.63	68.09	96.10	65.55	−100
ZnO/Cr_2O_3[a]	2.12	3.25	4.72	7.20	60.7	94.7	58.16	−119
$ZnO/MnSO_4$	0.31	0.33	0.36	0.38	10.30	101	7.76	−305
$ZnO/Fe_2(SO_4)_3$	0.74	0.88	1.01	1.23	27.00	98.4	24.46	−242

[a] Calcinated for three hours at 500°C

Calcination of $ZnO/CuSO_4$ and $ZnO/Cr_2(SO_4)_3$ catalysts for three hours at 500°C considerably increased their activity towards hydrogen peroxide decomposition (Table 2). This may be due to the transformation of some of the absorbed metal ions to the corresponding metal oxides. The colour changed from blue to gray and from gray to black for copper and chromium catalysts, respectively. These oxides may have a higher activity towards H_2O_2. This explanation is evidenced by EDX measurements which showed an increase in the content of the supported metal and a decrease in oxygen content on the surface of the catalyst upon calcination (Table 1) as well as by the XRD diffraction peaks recorded for the calcinated samples (Fig. 2). Earlier investigations have shown that the calcinated copper on zinc oxide-catalyst contains Cu^{2+} in a CuO-like phase as well as in substitutional sites in the ZnO lattice [38, 39].

The brown coloured intermediate formed by interaction of H_2O_2 with ZnO/Cu^{2+} was isolated from the reaction medium and investigated by EDX and FTIR (not included). EDX measurements revealed an increase in the oxygen content from 18.38 to 24.88%. On the other hand, FTIR spectra showed a more intense band in the region of antisymmetric and symmetric OH stretching modes (3500–3200 cm^{-1}) as well as a new band at 1400 cm^{-1} corresponding to δ vibrations of the hydrogen moiety [40].

The activation parameters were determined and are listed in Table 2. A plot of enthalpy *vs*. entropy change, (isokinetic relationship [39]) gave a straight line with slope equal to 290 K (Fig. 4). This isokinetic temperature is lower than the average experimental temperature (305.5 K). This means that the decomposition of H_2O_2 over these catalysts is entropy controlled, *i.e*. higher rates are associated with low entropies [17, 21]. The existence of an isokinetic relationship supports the claim that a single mechanism operates along the catalyst series [17, 20, 41].

The effect of pH on the reaction rate was studied at constant concentration of both the catalyst and H_2O_2 at 35°C. The rate of reaction increases with increasing pH and follows an S-shaped curve (Fig. 5). This rate enhancement is expected due

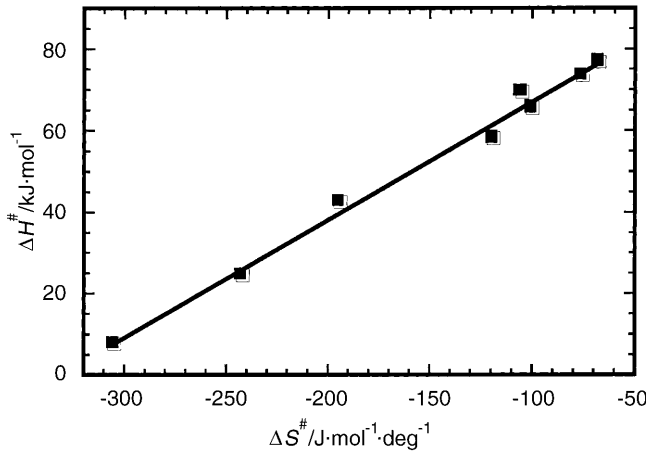

Fig. 4. Isokinetic relationship for the reaction of different catalysts with hydrogen peroxide

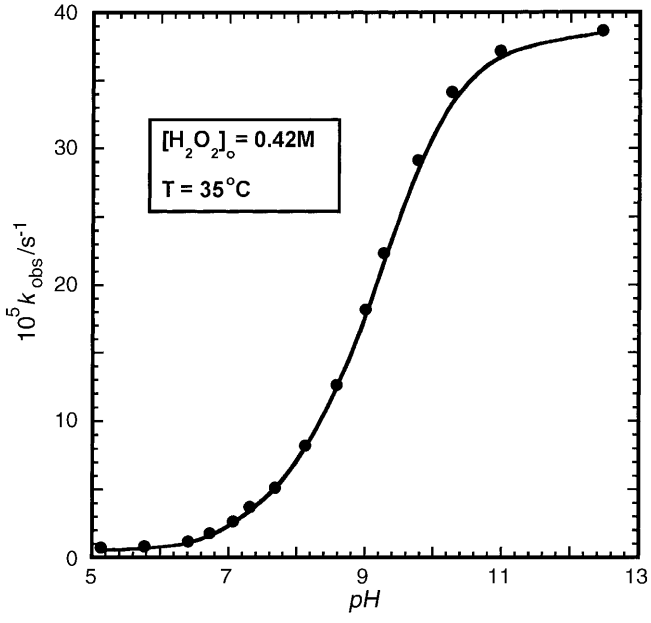

Fig. 5. Dependence of the observed rate constant on *pH* for the decomposition of hydrogen peroxide over one gram of ZnO/Cu^{2+} catalyst

to the enhanced deprotonation of H_2O_2 and, in turn, the enhanced formation of the peroxo-intermediate in alkaline solution [13, 21].

Before proposing a reaction mechanism, we have to point out that the decomposition rate of H_2O_2 is decreased by 27% in presence of 20% *t*-butanol as scavenger. This suggests the involvement of free radicals in the reaction scheme [24, 42].

According to the above observations and discussions, the following mechanism is proposed in which the location of the rate-determining step depends on the concentration range of H_2O_2 used:

$$\mathrm{ZnO}/M^{n+} + \mathrm{H_2O_2} \overset{K_1}{\rightleftharpoons} \underset{\text{peroxo intermediate}}{\mathrm{ZnO}/M^{n+}(\mathrm{HO_2})^-} + \mathrm{H^+} \xrightarrow[\text{slow}]{k_1} \mathrm{ZnO}/M^{(n-1)+} + \mathrm{HO_2^\bullet} \tag{1}$$

$$\mathrm{HO_2^\bullet} + \mathrm{H_2O_2} \rightarrow \mathrm{OH^\bullet} + \mathrm{O_2} + \mathrm{H_2O} \tag{2}$$

$$\mathrm{ZnO}/M^{(n-1)+} + \mathrm{OH^\bullet} \rightarrow \mathrm{ZnO}/M^{n+} + \mathrm{OH^-} \tag{3}$$

$$\mathrm{OH^-} + \mathrm{H^+} \rightarrow \mathrm{H_2O}$$

From Eq. (1), the concentration of the peroxo intermediate is given by

$$[\mathrm{ZnO}/M^{n+}(\mathrm{HO_2})^-] = K_1[\mathrm{ZnO}/M^{n+}][\mathrm{H_2O_2}]/[\mathrm{H^+}] \tag{4}$$

From

$$[\mathrm{H_2O_2}] = [\mathrm{H_2O_2}]_\mathrm{o} - [\mathrm{ZnO}/M^{n+}(\mathrm{HO_2})^-] \tag{5}$$

and

$$[\mathrm{ZnO}/M^{n+}] = [\mathrm{ZnO}/M^{n+}]_\mathrm{o} - [\mathrm{ZnO}/M^{n+}(\mathrm{HO_2})^-] \tag{6}$$

one obtains

$$\begin{aligned}[\mathrm{H_2O_2}][\mathrm{ZnO}/M^{n+}] = {} & [\mathrm{H_2O_2}]_\mathrm{o}[\mathrm{ZnO}/M^{n+}]_\mathrm{o} - [\mathrm{H_2O_2}]_\mathrm{o}[\mathrm{ZnO}/M^{n+}(\mathrm{HO_2})^-] \\ & - K_1[\mathrm{ZnO}/M^{n+}]_\mathrm{o}[\mathrm{ZnO}/M^{n+}(\mathrm{HO_2})^-] + [\mathrm{ZnO}/M^{n+}(\mathrm{HO_2})^-]^2\end{aligned}$$

The last squared term is very small compared to the others and can be neglected for simplification. Therefore, from this equation and Eq. (4), the concentration of the peroxo intermediate can be estimated as

$$[\mathrm{ZnO}/M^{n+}(\mathrm{HO_2})^-] = \frac{K_1[\mathrm{ZnO}/M^{n+}]_\mathrm{o}[\mathrm{H_2O_2}]_\mathrm{o}}{K_1([\mathrm{H_2O_2}]_\mathrm{o} + [\mathrm{ZnO}/M^{n+}]_\mathrm{o}) + [\mathrm{H^+}]} \tag{7}$$

Therefore the reaction rate is equal to

$$V = k_1[\mathrm{ZnO}/M^{n+}(\mathrm{HO_2})^-] = \frac{k_1K_1[\mathrm{ZnO}/M^{n+}]_\mathrm{o}[\mathrm{H_2O_2}]_\mathrm{o}}{K_1([\mathrm{H_2O_2}]_\mathrm{o} + [\mathrm{ZnO}/M^{n+}]_\mathrm{o}) + [\mathrm{H^+}]} \tag{8}$$

Equation (8) predicts that the reaction rate increases with increasing $[\mathrm{H_2O_2}]_\mathrm{o}$ at constant catalyst concentration attaining a limiting rate at relatively high values of $[\mathrm{H_2O_2}]_\mathrm{o}$. The reciprocal of this equation can be written as

$$\frac{1}{V} = \frac{1}{k_1[\mathrm{ZnO}/M^{n+}]_\mathrm{o}} + \frac{(K_1[\mathrm{ZnO}/M^{n+}]_\mathrm{o} + [\mathrm{H^+}])}{k_1K_1[\mathrm{ZnO}/M^{n+}]_\mathrm{o}[\mathrm{H_2O_2}]_\mathrm{o}} \tag{9}$$

From the intercept and the slope of a plot of $1/V$ *vs.* $1/[\mathrm{H_2O_2}]_\mathrm{o}$ (Fig. 6) one can estimate some tentative values of k_1 and K_1 (Table 3). However, Eqs. (8) and (9) cannot explain the decrease in rate at higher $[\mathrm{H_2O_2}]_\mathrm{o}$. In order to account for such a

decrease we propose that the reaction proceeds *via* the formation of a second intermediate:

$$\begin{aligned} &ZnO/M^{n+}(HO_2)^- + H_2O_2 \overset{K_2}{\rightleftharpoons} ZnO/M^{n+}(HO_2)^-H_2O_2 \\ &\text{peroxo-intermediate} \\ &\qquad \xrightarrow[\text{slow}]{k_2} ZnO/M^{(n-1)+} + O_2 + H_2O + HO^\bullet \end{aligned} \tag{10}$$

The concentration of the second intermediate is given by

$$[ZnO/M^{n+}(HO_2)^-(H_2O_2)] = K_2[ZnO/M^{n+}(HO_2)^-][H_2O_2] \tag{11}$$

From Eqs. (11) and (4) one obtains

$$[ZnO/M^{n+}(HO_2)^-(H_2O_2)] = K_1K_2[ZnO/M^{n+}][H_2O_2]^2/[H^+]$$

Substitution from Eqs. (5) and (6) affords

$$[ZnO/M^{n+}(HO_2)^-(H_2O_2)] = \frac{K_1K_2([ZnO/M^{n+}]_o[H_2O_2]_o^2 - 2[ZnO/M^{n+}]_o[H_2O_2]_o[ZnO/M^{n+}(HO_2)^-]_o)}{[H^+]} \tag{12}$$

A combination of Eqs. (12) and (7) then yields

$$[ZnO/M^{n+}(HO_2)^-(H_2O_2)] = \frac{K_1^2K_2[ZnO/M^{n+}]_o[H_2O_2]_o^3 + K_1K_2[H]^+ - K_1^2K_2[ZnO/M^{n+}]_o^2[H_2O_2]_o^2}{K_1[H^+]([H_2O_2]_o + [ZnO/M^{n+}]_o)} \tag{13}$$

Since $K_1 = 1.5 \times 10^{-12}\,\text{mol} \cdot \text{dm}^{-3}$ at 30°C [43], K_1^2 is in the range of $10^{-24}\,\text{mol}^2 \cdot \text{dm}^{-6}$. Therefore, the first and the last terms in the numerator are very small compared to the middle one and can be omitted. Equation (13) then turns into

$$[ZnO/M^{n+}(HO_2)^-(H_2O_2)] = \frac{K_2}{([H_2O_2]_o + [ZnO/M^{n+}]_o)}, \tag{14}$$

and the rate equation becomes

$$V = k_2[ZnO/M^{n+}(HO_2)^-(H_2O_2)] = \frac{k_2K_2}{([H_2O_2]_o + [ZnO/M^{n+}]_o)} \tag{15}$$

Table 3. Estimated K_1 and k_1 for the reaction of different catalysts with hydrogen peroxide at 35°C and $pH = 8.15$

Catalyst	Estimated values	
	$10^{-6}\ K_1$	$10^2\ k_1$
$ZnO/CuSO_4$	4.0	1.00
$ZnO/CoSO_4$	12.5	1.25
$ZnO/NiSO_4$	426	5.10
$ZnO/Cr_2(SO_4)_3$	0.2	0.31
$ZnO/MnSO_4$	67.0	4.30
$ZnO/Fe_2(SO_4)_3$	1.5	1.00

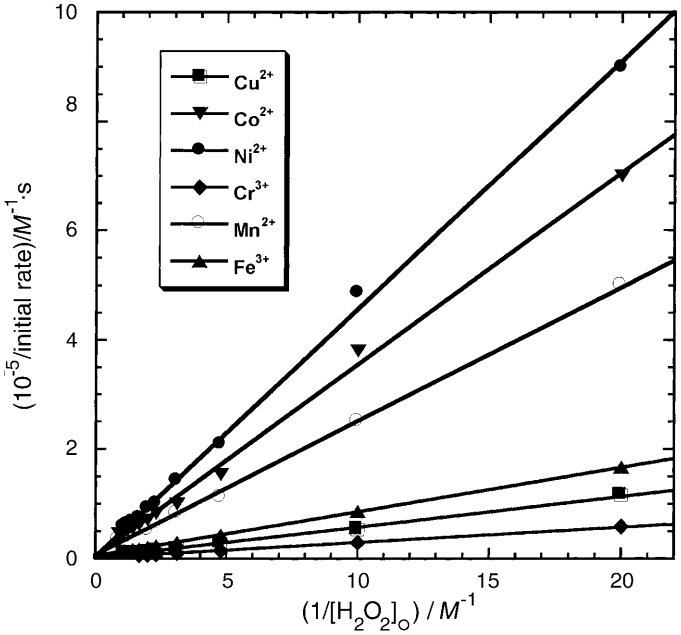

Fig. 6. Reciprocal of initial rate *vs*. reciprocal $[H_2O_2]_o$ for the reaction of two grams of loaded ZnO with H_2O_2 at 35°C and $pH = 8.15$

Now it is clear that at constant catalyst concentration the rate of reaction decreases with increasing $[H_2O_2]_o$ (the last part of the curves in Fig. 3). On the other hand, Eq. (8) can also explain the *pH* dependence shown in Fig. 5. With increasing $[H^+]$, *i.e*. decreasing *pH*, the rate is inversely proportional to $[H^+]$. However, at higher *pH*, $[H^+]$ can be omitted from the denominator, and the reaction rate becomes independent on *pH*. The rate equation then becomes

$$V = \frac{k_1[\mathrm{ZnO}/M^{n+}]_o[H_2O_2]_o}{[H_2O_2]_o + [\mathrm{ZnO}/M^{n+}]_o} \tag{16}$$

Conclusions

Pure ZnO has almost no catalytic activity towards H_2O_2 decomposition. However, loading ZnO with some transition metal sulfates, *e.g*. $CuSO_4$, $CoSO_4$, $NiSO_4$, $Cr_2(SO_4)_3$, $MnSO_4$, and $Fe_2(SO_4)_3$ increases its activity. The catalytic activity depends on the amount of supported metal ion, its redox potential, and the pH value. The order of reactivity of the supported catalysts depends on the hydrogen peroxide concentration. Calcination of copper and chromium catalysts at 500°C considerably increases their activity; this is ascribed to the formation of the corresponding metal oxides. Preliminary experiments (not included) showed that the free radicals formed from the interaction of H_2O_2 with these catalysts are able to oxidize and decolourize some organic dyes that can be found in textile waste effluents. These reactions are currently under investigation.

Experimental

Materials and reagents

All chemicals were of analytical reagent grade quality (Merck). H_2O_2 solutions were prepared by direct dilution and standardized iodometrically using sodium thiosulfate.

Metal ions supported on zinc oxide

Zinc oxide from Merck (particle size *ca.* 0.5–2 mm) was washed repeatedly with redistilled H_2O, dried, and activated at 150°C for 24 h. The required amount of activated ZnO was kept in contact with excess solution of metal sulfate (10^{-3} *M*, 1 dm^3) for 24 h at room temperature with continuous stirring [44]. Successive additions of the metal sulfate solution were performed until the metal ion was detected in the external solution. The loaded ZnO (ZnO/M^{n+}) was then filtered, washed repeatedly with redistilled H_2O until free from any excess of metal sulfate solution, and dried at 150°C.

Physical measurements

An atomic absorption spectrometer 906 GBC AA with a graphite furnace (GF 3000) and hydride generator (HG 3000) was used to determine the amount of metal ions adsorbed per gram of catalyst. This was done after leaching the supported metal ions with dilute nitric acid solution. The amount (mg) of metal ion per g catalyst for the different catalysts is listed in Table 1. A Philips X-ray diffractometer model PW/1840 (Ni filter, CuK_α radiation ($\lambda = 1.542$ Å), 40 kV, 30 mA, scanning speed 0.02°/s was used for XRD measurements. High resolution scanning electron micrographs (SEM) and energy dispersive X-ray (EDX) measurements were carried out with a Jeol scanning electron microscope JSM-5600 equipped with an energy dispersive X-ray ISIS OXFORD instrument. FTIR measurements were performed with a Nicolet FT-IR Magna-IR 560 spectrometer. *pH* measurements were done employing a Mettler Delta 320 *pH*-meter, and phosphate buffer was used throughout. For high *pH* values, few drops of sodium hydroxide were added.

Kinetic measurements

Kinetic measurements were carried out following a procedure described previously [20, 22] in the range of 25–40°C. The observed rate constant, k_{obs}, was evaluated from the integrated first order equation. The initial reaction rate values were determined from the extrapolation of straight lines of $d[H_2O_2]/dt$ *vs.* $[H_2O_2]$ plots.

Acknowledgements

The Scientific Research Council of the United Arab Emirates University funded this research work.

References

[1] Prengle HW Jr Symons JM, Belhateche D (1996) Waste Management **16**: 327
[2] Parvulescu VI, Dumitriu D, Poncelet G (1999) J Mol Catal **140**: 91
[3] Centi G, Perathoner S, Torre T, Verduna MG (2000) Catal Today **55**: 61
[4] Pestunova OP, Elizarova GL, Parmon VN (1999) Russ J Appl Chem **72**: 1147
[5] Dionysiou DD, Suidan M, Bekou E, Baudin I, Laine JM (2000) Appl Catal B **26**: 153
[6] Fischer J, Holderich WF (1999) Appl Catal A **180**: 425
[7] Leitner NKV, Dore M (1996) J Photochem Photobiol **99**: 137

[8] Spadaro JT, Isabelle L, Renganathan V (1994) Environ Sci Technol **28**: 1389
[9] De AK, Chaudhuri B, Bhattacharjee S, Dutta BK (1999) J Hazard Mater B **64**: 91
[10] Porter JJ, Walsh WK (1995) National Textile Center Annual Report **A92-4**: 17
[11] Colonna GM, Caronna T, Marcandalli B (1999) Dyes Pigments **41**: 211
[12] Wu K, Xie Y, Zhao J, Hidaka H (1999) J Mol Catal **144**: 77
[13] Salem I, Elmazawy MS (2000) Chemosphere **41**: 1173
[14] Chen F, Doong RA, Lei WG (1998) Water Sci Tecnol **37**: 187
[15] Stoffler B, Luft G (1999) Chemosphere **38**: 1035
[16] Kholdeeva OA, Maksimov GM, Moksimovskaya RI, Kovaleva LA, Fedotov MA (1999) React Kinet Catal Lett **66**: 311
[17] Selvaraj PC, Mahadeva V (1997) J Mol Catal A **120**: 47
[18] Deshmukh AP, Akerkar VG, Salunkhe MM (2000) J Mol Catal A **153**: 75
[19] Prasad RV, Thakkar NV (1994) J Mol Cat **92**: 9
[20] Gemeay AH (1996) Colloids Surface A **116**: 277
[21] Oliveira SF, Espinola JGP, Lemus WES, de Souza AG, Airoldi C (1998) Colloids Surface A **136**: 151
[22] Gemeay AH, Salem MA, Salem IA (1996) Colloids Surface A **117**: 245
[23] Barrault J, Bouchoule C, Echachoui K, Frinisrasra N, Trabelsi M, Bergaya F (1998) Appl Catal B **15**: 269
[24] Salem IA, El-Hag RI, Khalil KMS (2000) Transition Met Chem **25**: 260
[25] Hasan MA, Zaki MI, Posupulety L, Kumari K (1999) Appl Catal A **181**: 171
[26] Lin SS, Gurol MD (1998) Environ Sci Technol **32**: 1417
[27] Chou SS, Huang CP (1999) Chemosphere **38**: 2719
[28] Fagal GA, Attia AA, El-Shobaky HG (1998) Ads Sci & Technol **16**: 381
[29] Drijvers D, Vanlangenhove H, Beckers M (1999) Water Research **33**: 1187
[30] Selim MM, El-Aiashi MK, Mazhar HS, Kamal SM (1996) Mater Lett **28**: 417
[31] Kirillov VA, Kuzin NA, Gavrilin VN, Kuz'min VA (1995) Kinet Catal **36**: 616
[32] El-Shobaky GA, Radwan NRR, Radwan FM (1998) Ads Sci & Technol **16**: 733
[33] Villasenor J, Reyes P, Pecchi G (1998) J Chem Technol Biotechnol **72**: 105
[34] Klenov DO, Kryukova GN, Plyasova LM (1998) J Mater Chem **8**: 1665
[35] El-Shobaky HG, Mokhtar M, El-Shobaky GA (1999) Appl Catal A **180**: 335
[36] Peralta-Zamora P, de Moraes SG, Pelegrini R, Freire M, Reyes J, Mansilla H, Duran N (1998) Chemosphere **36**: 2119
[37] Kotrly S, Sucha L (1985) Handbook of Chemical Equilibria in Analytical Chemistry. Ellis Horwood, Chichester, chapt 9, p 221
[38] Sankar G, Vasudevan S, Rao CNR (1986) J Chem Phys **85**: 2291
[39] Arunakavalli T, Kulkarni GU, Rao CNR (1993) Catal Lett **20**: 259
[40] Nakamoto K (1963) Infrared Spectra of Inorganic and coordination Compounds, part III. Wiley, New York, p 156
[41] Espenson JH (1995) Chemical Kinetics and Reaction Mechanism, 2nd edn. McGraw-Hill, New York, chapt 7, p 164
[42] Rush JD, Koppenol WH (1987) J Inorg Biochem **29**: 199
[43] Sreekala R, Yusuff KKM (1995) Ind J Chem A **34**: 994
[44] Brunelle JP (1979) In: Delmon B, Grange P, Jacobs PA, Poncelet G (eds) Preparation of Catalysts, vol II. Elsevier, Amsterdam, p 211

Received April 26, 2000. Accepted (revised) August 24, 2000